RSC Advances

This is an *Accepted Manuscript*, which has been through the Royal Society of Chemistry peer review process and has been accepted for publication.

Accepted Manuscripts are published online shortly after acceptance, before technical editing, formatting and proof reading. Using this free service, authors can make their results available to the community, in citable form, before we publish the edited article. This *Accepted Manuscript* will be replaced by the edited, formatted and paginated article as soon as this is available.

You can find more information about *Accepted Manuscripts* in the **Information for Authors**.

ROYAL SOCIETY
OF CHEMISTRY

www.rsc.org/advances

Au nanoparticle-embedded SiO₂-Au@SiO₂ catalysts with improved catalytic activity, enhanced stability to metal sintering and excellent recyclability

Uiseok Jeong[1], Ji Bong Joo[2]*, Younghun Kim[1]*

[1]Department of Chemical Engineering, Kwangwoon University, Seoul, 139-701, Republic of Korea

[2]Low Carbon Process Lab, Korea Institute of Energy Research, Deajeon, 305-343, Republic of Korea

*Corresponding authors (Tel: +82-42-860-3019, E-mail: jbjoo@kier.re.kr, Tel: +82-2-940-5768, E-mail: korea1@kw.ac.kr)

Abstract

Synthesizing a precious metal catalyst with high performance and excellent recyclability is always an important issue in catalysis. Here, we report a synthetic strategy for preparing gold nanoparticle (Au NP)-embedded SiO₂ particles for use as recyclable nanocatalysts. Au NP-embedded SiO₂ (SiO₂-Au@SiO₂) particles were synthesized by applying Au NP decoration on the surface of the SiO₂ particles and additional SiO₂ coating through sol-gel reaction. In order to improve molecule accessibility, catalyst stability and

catalytic performance, post-treatments such as calcination and/or etching with water or ammonia were carried out. Systemic study on the physical property changes of the resulting SiO_2-Au@SiO_2 samples with variation on each synthetic step revealed that couples of parameters that are very important for determining the catalytic performance, namely Au NP stability, porosity and capping agent on the Au surface, are strongly influenced by each post-treatment step. In particular, calcination followed by etching with ammonia enables the production of a highly active SiO_2-Au@SiO_2 catalyst with highly dispersed Au NPs in the silica layer, a surfactant-free Au surface and an improved porosity of the silica layer, which displays significantly enhanced catalytic performance and excellent recyclability as compared to SiO_2-Au and as-synthesized SiO_2-Au@SiO_2.

1. INTRODUCTION

Metal nanostructures have attracted interest since several pioneering works elucidated that nanoscale metal particles can have unique optical, physical, chemical, catalytic and electrochemical properties that are not observed on bulk counterparts.[1-10]. Bulk gold (Au) is a stable and inert precious metal.[11, 12] As the diameter of the Au particle continuously deceases to less than a certain size, it eventually loses its bright-shiny gold color and gains different colors, indicating a change in its chemical and optical properties. In addition, it has rarely been used as an active material such as a catalyst because Au has been considered a fairly inert and catalytically inactive metal.[11-13] However, since Haruta et al. first demonstrated the exceptional reactivity of small Au nanoparticles (NPs) dispersed on suitable substrates,[14-16] numerous reports have been published on Au catalysis for the promotion of a variety of chemical reactions.[17-22]

Over the past decade, intensive efforts have focused on synthesizing nanoscale materials and remarkable progress has been achieved on the fabrication of novel nanomaterials.[23-29] With continuous development in synthetic chemistry for Au nanostructures, a new class of well-defined Au NPs, that are uniform, shape-controlled, and size-tuned, has been fabricated and evaluated in many practical applications.[30-32] Especially, since the discovery of the outstanding performance of Au NPs in catalysis,[14-16] researchers have synthesized well-defined Au NPs that can be used in many catalytic reactions.[17, 22, 33-35]

It could be thought that pre-synthesized Au NPs can be directly used as an active catalyst in liquid phase catalysis. Although colloidal Au NPs have advantageous characteristics for liquid phase catalysis, the capping ligand, which can stabilize Au NPs, not only limits the access of the reactant to the active site but also hampers the surface reaction. In addition, if the capping agents are removed from the Au surface, NPs tend to be aggregated and/or change their shapes because of their high surface energies, leading to losing their unique

activity.

Traditionally, supporting active metal particles on suitable support materials followed by calcination has been a common method to synthesize highly dispersed metal catalysts having clean active surface.[36, 37] Pre-synthesized Au NPs can also be supported on the surface of suitable support materials such as silica and titania through surface functionalization, direct anchoring and calcination. Despite few studies on the synthesis of supported Au catalysts with uniform particle dimension, high dispersion and clean active site,[38-40] pre-synthesized Au NPs are generally deformed and sintered during the calcination step.

Recently, it has been realized that metallic NPs can be stabilized against thermal sintering by encapsulating the metal particle within an inorganic layer to form a core-shell nanostructure.[33, 41-44] So far, many pioneering studies have successfully demonstrated encapsulating metal NPs with SiO_2, TiO_2, carbon and polymers.[18, 33, 35, 43, 44] In the molecular diffusion point of view, the dense inorganic layers, unfortunately, hinder reactant molecules from reaching the buried metal and limit catalysis. Consequently, an ideal structure needs to be designed to satisfy the following requirement: An additional shell layer should protect each embedded metal particle from thermal metal sintering and allow reactant molecules to access the active metal surface. Ideally, encapsulation with a porous layer can keep metal NPs stable even during high temperature calcination conditions and allow the reactant molecules to access the surface of the embedded metal particles.[44, 45] As representative examples, Liz-Marzan and co-workers demonstrated a hybrid composite material which is sub-monolayer of Au NPs with various shapes covered with mesoporous silica thin film.[46, 47] They first anchored the Au NPs on the glass substrate and deposited mesoporous silica thin film. Mesoporous silica film can allows Au precursors to diffuse into the embedded Au NPs and Au NPs can be grown to various shapes. Corma and co-workers developed a neat concept for formation of mesoporous silica layer on Au NPs through deposition of nonporous silica

followed by pseudomorphic transformation of amorphous silica.[48, 49] They successfully achieved Au NPs-mesoporous silica composites with high surface area, controlled the important properties such as the number of Au NP core and investigated optical characteristic changes. Although previous pioneering works considered different goals on various applications, they can give us important insight on designing Au NP catalysts with high performance and excellent stability.

In this work, we synthesized Au NP-embedded SiO_2-Au@SiO_2 catalysts and controlled the porosity of the outer silica shell through various post-treatments such as calcination and/or etching with water or aqueous ammonia. We systemically characterized the physical properties of the SiO_2-Au@SiO_2 samples and evaluated their catalytic performances on 4-nitrophenol (4-NP) reduction. As discussed later, it can be expected that post-treatments used in this work not only convert the solid silica shell into the porous counterpart but also remove the surface surfactant on the Au surface without metal sintering. Thus, the resulting SiO_2-Au@SiO_2 sample can show relatively high catalytic performance, enhanced metal stability and excellent recyclability. Our results could provide a good example for the synthesis of novel nanocatalysts having advantageous characteristics such as sintering-resistant active metal with high catalytic recyclability.

2. EXPERIMENTAL SECTION

2.1. Materials and Chemicals.

Hydrogen tetrachloroaurate (III) hydrate (HAuCl$_4$, $\geq$ 49% Au basis) was purchased from KOJIMA chemicals. Ethanol (C$_2$H$_5$OH, 99.9%) and ammonium hydroxide (NH$_4$OH, 28%) were obtained from Duksan Chemical company. Trisodium citrate dihydrate (TSC, 99%), polyvinylpyrrolodone (PVP, Mw= ~10,000), and (3-aminopropyl)triethoxysilane (APTES, 98%) were purchased from Sigma-Aldrich. Tetraethyl orthosilicate (TEOS, 99%) was

obtained from Aldrich. Sodium borohydride (NaBH$_4$ 99%) was obtained from Fluka. 4-nitrophenol (4-NP, 98%) was purchased from Samchun Chemicals. All chemicals were used as received without further treatment

2.2. Synthesis of Au nanoparticles (NPs)

Small Au NPs were prepared by conventional chemical reduction method[30]. Briefly, an aqueous solution of HAuCl$_4$ (2.5 mM, 2mL) and TSC (5 mM, 1 mL) was added to deionized water (DI water, 17 mL) at atmosphere conditions and the resulting mixture was kept for 10 min under vigorous stirring. An aqueous NaBH$_4$ solution (100 mM, 0.6 mL) was quickly injected into the mixture and the solution was aged for 30 min. The yellow color of the Au precursor solution rapidly changed to a reddish color right after addition of the NaBH$_4$ solution, indicating that Au^{3+} ions were reduced to form small Au NPs. Next, an aqueous solution of PVP (0.2 g/mL, 0.5 mL) was added to the above Au NP solution for 1h at room temperature and the solution was kept in a refrigerator for further use.

2.3. Synthesis of Au NP-embedded SiO$_2$-Au@SiO$_2$ composites

Au NP-embedded SiO$_2$-Au@SiO$_2$ nanocomposites were prepared by decorating pre-synthesized Au NPs on the surface of SiO$_2$ particles, followed by sequential coating with an additional SiO$_2$ layer. Spherical SiO$_2$ particles were synthesized by Stöber method[50]. TEOS (1 mL), DI water (24.75 mL) and aqueous NH$_4$OH solution (6 mL) were sequentially added to ethanol (16.25 mL) and the mixture was stirred continuously at atmosphere conditions for 4 hr. The precipitated SiO$_2$ particles were separated by centrifugation, washed 3 times with ethanol, and then redispersed in 15 mL ethanol. To functionalize the silica surface with an amine group, we carried out APTES functionalization. The above silica solution (5 mL) was well dispersed in ethanol (15 mL) by ultrasonication. APTES (0.2 mL) was added to the silica

solution under vigorous stirring and the mixture was stirred continuously for 6 hr to ensure complete functionalization on the silica surface. The precipitated APTES-SiO$_2$ samples were separated by centrifugation and washed 3 times with ethanol, and then redispersed in ethanol (20 mL).

APTES-functionalized SiO$_2$ (5mL) was then injected into the pre-synthesized Au solution (20 mL) under vigorous stirring and the mixture was stirred continuously overnight. During stirring, a change in the white color of the silica particles to red color indicates Au NP adsorption on the surface of silica. The resulting red precipitates were isolated by centrifugation, washed 3 times with ethanol, and then redispersed in ethanol (20 mL) to give SiO$_2$-Au sample. For purpose of estimating metal content, some portion of SiO$_2$-Au sample is well dried in the convection oven at 90 ^{o}C for 6 hr and it displays ca. 1.7 wt% of Au content by ICP-OES analysis.

To coat an outer silica layer on the SiO$_2$-Au, sol-gel coating was carried out again.[27] The above SiO$_2$-Au particles were dispersed in the ethanol and TEOS (0.2 mL), DI water (5 mL) and NH$_4$OH (1 mL) were sequentially added into the solution. After stirring for 4 h, SiO$_2$-Au@SiO$_2$ samples were collected by centrifugation, washed three times with ethanol and water, and redispersed in 20 mL water. For purpose of estimating metal content, some portion of SiO$_2$-Au@SiO$_2$ sample is well dried in the convection oven at 90 ^{o}C for 6 hr and it shows ca. 1wt% of Au content by ICP-OES analysis.

2.4. Etching of SiO$_2$-Au@SiO$_2$ with water

The prepared SiO$_2$-Au@SiO$_2$ (10 mL) sample was heated at 95 ^{o}C for 1h and the solution was cooled down to room temperature. After water etching, the sample was finally collected by centrifugation, washed and redispersed in ethanol (10 mL) for characterization and catalysis experiments. The sample is denoted as SiO$_2$-Au@SiO$_2$-H$_2$O.

2.5. Etching of SiO$_2$-Au@SiO$_2$ with weak-base solution

The prepared SiO$_2$-Au@SiO$_2$ (10 mL) sample was mixed with aqueous NH$_4$OH solution (5.6%, 10mL) and stirred for 1 h with vigorous stirring at ambient conditions. The etched particles were washed and finally dispersed in ethanol (10 mL) for further experiments. The sample is denoted as SiO$_2$-Au@SiO$_2$-NH$_3$.

2.6. Calcination of SiO$_2$-Au@SiO$_2$

The prepared SiO$_2$-Au@SiO$_2$ (10 mL) sample was dried at 60 $^{\circ}$C under vacuum conditions for 12 h, calcined at the desired temperature (450 $^{\circ}$C) in air for 1h with a ramping rate of 10 $^{\circ}$C/min, and redispersed in ethanol (10 mL) for further experiments. The sample is denoted as SiO$_2$-Au@SiO$_2$-Cal.

2.7. Calcination followed by etching of SiO$_2$-Au@SiO$_2$

The above calcined SiO$_2$-Au@SiO$_2$ sample (10 mL) was mixed with aqueous NH$_4$OH solution (5.6%, 10 mL), stirred for 1 h under vigorous stirring at ambient conditions, washed and finally redispersed in ethanol (10 mL) for further experiments. The sample is denoted as SiO$_2$-Au@SiO$_2$-Cal-NH$_3$.

2.8. Characterization

The morphology, particle dimension, and dispersion degree of the prepared samples were investigated by transmission electron microscopy (TEM, JEOL JEM-2010). The surface areas of the prepared samples were calculated by the Brunauer-Emmett-Teller (BET) equation with data obtained by N$_2$ adsorption isotherms experiment at 77 K (Micrometrics ASAP 2010 sorption instrument). Pore size distributions were calculated by the BJH method using

adsorption branches of each N_2 isotherm. The UV-Vis absorbance of the Au samples and concentration of 4-NP were measured by UV-Vis spectrophotometry (Shimazdu, UV-1800). Thermogravimetric analysis (TGA) was conducted by using a TGA instrument (TA instrument SDT Q600). TGA curves are reordered by continuous heating at a ramping rate of 5 ^{o}C/min from room temperature to 700 ^{o}C in air. In order to find loading amount of Au, Inductively Coupled Plasma Optical Emission Spectroscopy (ICP-OES) was conducted (PerkinElmer, Optima 2000DV).

2.9. Catalytic Reaction.

The catalytic performances of the prepared SiO_2-Au@SiO_2 samples were evaluated by reduction of 4-NP in the presence of $NaBH_4$ as a reducing agent. DI water (2 mL), aqueous 4-NP solution (10 mM, 0.01 mL) and $NaBH_4$ solution (0.1 M, 0.16 mL) were added into a quartz cuvette followed by the addition of the catalyst sample solution (0.2 mL, total amount of Au is ca 100 μg in the solution) to the above mixture to initialize the reaction. Catalytic efficiency was evaluated by calculating the degradation rate of 4-NP. The reaction progress was monitored by measuring the UV-vis absorption spectra of the reaction mixture to quantify the concentration of 4-NP in the solution.

3. RESULTS AND DISCUSSION

Colloidal Au NPs can be synthesized by various chemical reduction methods using Au precursor, a reduction agent and a capping agent.[18, 30, 31, 34, 39] Since smaller metal particles can provide larger specific active sites, we synthesized Au NPs with 3~5 nm diameter by $NaBH_4$ reduction method using Au precursor ($HAuCl_4$) with weak capping agent (TSC). Although TSC-stabilized Au NPs (Au NPs-TSC) can be dispersed in DI water, TSC-Au NPs can be easily aggregated by changing the solution environment. As shown in Figure S1(a), the original reddish color of the as-synthesized Au NPs-TSC solution was changed to dark violet by adding $NaBH_4$ solution (which is similar to the conditions of catalytic 4-NP reduction), indicating the instability of the Au NPs and their irreversible aggregation. The original UV-Vis absorption peak of the Au NP solution at 505 was shifted to 520 nm and became much smoother due to irreversible aggregation of small Au NPs.[51] Replacing TSC to other capping agents with strong interactions with the metal surface can improve the stability of metal NPs. Apparently, PVP treatment on the pre-synthesized Au NP solution can dramatically enhance the stability of Au NPs in the solution.[18, 34, 43, 45] The reddish color of the PVP-treated Au NPs (Au NPs-PVP) solution was maintained and the UV-Vis absorption peak shift of the Au NP solution was negligible even after adding $NaBH_4$ solution, indicating the well maintained stability (Figure S1(b)).

Another issue on colloidal NP catalysts is recyclability. Although well dispersed Au NPs can catalyze chemical reactions with high efficiency, the catalytic materials must be recovered through suitable separation methods and be recycled for further use. However, it is difficult to separate out well-dispersed Au NPs selectively, because their diameter is too small and the surface stabilizer ensures complete dispersion of the particles in the solution. As shown in Figure S2, although we tried to separate Au NPs out selectively by centrifugation under severe rotation conditions (13000 rpm for 30 min or 60 min), little Au NP was

collected and the color of the supernatant remained reddish, indicating that most of the Au NPs were still dispersed in the solution. In the UV-Vis spectra results, the absorbance peak change of each supernatant solution after centrifugation for different periods was negligible compared to that of the original PVP-treated Au NP solution.

In order to address both metal aggregation and recyclability issues, metal NPs are often deposited on suitable support materials such as SiO_2, Al_2O_3, and TiO_2 through various strategies. We also deposited pre-synthesized Au NPs on silica spheres as a support material and evaluated their catalytic properties and activities. In order to deposit Au NPs on the surface of the silica spheres, we first conducted surface functionalization to introduce amine groups that have a strong chemical interaction with Au NPs. Since SiO_2 spheres have many Si-OH groups on their surfaces, it can be expected that the surface is easily functionalized to have amine groups through APTES treatment. PVP-treated Au NP solution was then mixed with APTES-treated SiO_2 sphere solution and Au NPs were allowed to be adsorbed on the surface of SiO_2 to form SiO_2-Au samples. As shown in Figure 1(a), the SiO_2-Au sample showed well dispersed Au NPs on the silica surface. As shown in previous studies,[22, 33] and as discussed below, although the SiO_2-Au sample showed the most rapid kinetics on 4-NP reduction, most of the Au NPs could be detached through the multiple recycling processes, indicating that the interaction between the SiO_2 surface and the Au NPs was insufficiently strong to anchor the Au NPs permanently. As shown in Figure 1(b), only a couple of Au NPs were observed on the surface of the SiO_2 sphere after 5 catalysis runs, indicating that most of the Au NPs were detached and washed out during repeated reaction runs and washing processes. To induce a strong interaction between metal particles and the surface of support materials, thermal treatment (i.e., calcination) can be considered. Thermal treatment also decomposes surfactant molecules (e.g., PVP) to clean the metal surface. However, thermal treatment sometimes induces surface migration of metal NPs for sintering into larger particles.

As shown in Figure 1(c), Au NPs were sintered to become larger particles after calcination at 450 $^{\circ}$C, which reduced the large active surface area and lost the unique catalytic activity. In order to address these two issues, we therefore proposed the introduction of a porous shell layer to allow reactant molecules to diffuse in and to prevent the sintering of Au particles even after high temperature calcination. Indeed, a porous shell improved the catalyst characteristics in terms of particle detachment, metal sintering and catalyst recyclability, with considerably high catalytic activity as discussed below.

An additional porous silica layer can be introduced on the surface of the pre-synthesized SiO_2-Au sample by sol-gel coating of solid silica layer, followed by etching with various methods to generate nanoscale pores in the outer shell. Scheme 1 shows a schematic illustration of the preparation procedures for the SiO_2-Au@SiO_2 samples at each synthetic step. After coating the SiO_2-Au sample with a solid silica layer, we applied several different post-treatments such as water etching, calcination and calcination followed by etching to generate nanoscale porosity and/or to remove the surfactant stabilizer (PVP) on the Au surface.

Figure 2 shows a TEM image of the as-synthesized SiO_2-Au@SiO_2 sample and corresponding catalytic performance result on 4-NP reduction. The as-synthesized SiO_2-Au@SiO_2 particle shows the evenly distributed and embedded Au NPs without any particle aggregation in the silica sphere, indicating that the catalytically active Au surface is covered by an outer silica layer (Figure 2a). Practically, when the as-synthesized SiO_2-Au@SiO_2 sample was used as a catalyst in 4-NP reduction, the conversion efficiency was dramatically decreased, compared to results of SiO_2-Au and other SiO_2-Au@SiO_2 catalysts after post-treatment, as discussed below (Figure 2b). The silica layer formed by sol-gel chemistry contains micropores with size of several angstroms that can effectively prevent the permeation of molecules and ions.[27, 33, 45, 52, 53] Due to existence of the solid silica layer

covering the Au NPs in the sample, the reactant (4-NPs) molecules should have difficulty to access the surface of the embedded Au NPs, resulting in the low catalytic efficiency.

To improve the accessibility of reactant molecules to Au particles through the outer silica layer, we carried out silica etching by using a couple of etching agents. Strong base chemicals such as NaOH and KOH can easily dissolve amorphous silica materials.[26, 28, 54-56] However, it has been troublesome to apply these strong base chemicals to create nanoscale pores in the outer silica layer selectively, because of the difficulty in precisely controlling the etching degree. Practically, a milder etching agent that can dissolve silica in a more controllable manner is required. Diluted ammonia solution is not a relatively strong base etchant but still has enough strength to dissolve amorphous silica colloids in controlled conditions. Water can also be considered as an one of the milder etchants.[44] Prior studies suggested that silica colloids prepared by a sol-gel process usually have an incompletely condensed surface because the interconnection of Si-O-Si bonds is highly disordered and discontinuous.[57] The silica can be re-dissolved in the form of monomeric $Si(OH)_4$ until the solubility equilibrium can be established when it is dispersed in even water.[58] In addition, ensuring a clean metal surface is also important to improve the accessibility and surface reaction. Calcination at a certain temperature is a simple method to burn out any remaining surfactant and clean the metal surface.[27] In practice, we conducted calcination to remove any surface surfactant, e.g., PVP, followed by sequential silica etching process by using a milder etchant.

TEM was used to determine the morphology changes in the SiO_2-Au@SiO_2 particles after each post-treatment, such as calcination and/or etching. As shown in Figure 3, the particle dimension and the spherical morphology are unchanged after each post-treatment, indicating that the particles were not severely etched out and that precisely controlled etching was achieved to form nanoscale pores in the silica particles during calcination and/or etching processes. When aqueous ammonia solution was used as an etchant, the SiO_2-Au@SiO_2

sample etched by ammonia (SiO_2-Au@SiO_2-NH_3) clearly showed couples of white pinholes, indicating that some silica was dissolved out to give a porous structure (Figure 3(a)). Although many Au particles with small diameter are observed in the silica particles, large Au particles are observed out of the silica particles (red circles). This indicates that diluted ammonia can dissolve some portion of silica severely and that several small Au particles are detached from the silica to be aggregated. It also means that as-synthesized silica is easily dissolved out even by mild base etchant (diluted ammonia solution). When the SiO_2-Au@SiO_2 sample was dispersed in water and etching was conducted at 95 ^{o}C for 1 hr (SiO_2-Au@SiO_2-H_2O), the morphological change was negligible, indicating that a small portion of the silica could be dissolved out (Figure 3(b)). Although no obvious change was evident in the TEM imaging, the physical properties must have been changed to give the improved catalysis performance when compared to the results of as-synthesized SiO_2-Au@SiO_2, as described below. As shown in Figure 3(c), when the SiO_2-Au@SiO_2 sample was calcined at 450 ^{o}C (SiO_2-Au@SiO_2-Cal), the sample also showed negligible change. Although it is hard to distinguish the morphology change in TEM imaging, the PVP surfactant covering the surface of the supported Au particles should be removed through high temperature calcination and molecular accessibility should be improved to give higher catalytic activity compared to that of original SiO_2-Au@SiO_2. When we carried out etching process toward the calcined SiO_2-Au@SiO_2 sample by using diluted ammonia solution, the sample (SiO_2-Au@SiO_2-Cal-NH_3) showed a porous morphology in the silica particle without any decrease of particle diameter. Despite the calcination and ammonia etching, the Au NPs embedded in the silica particle were not detached at all and remained in the silica particle, indicating that a small portion of silica was homogeneously dissolved out to form a porous structure. Even though the same etching conditions of diluted ammonia were used, severe silica etching didn't occur and all the Au NPs are remained in the silica particles in the case of SiO_2-Au@SiO_2-Cal-NH_3.

It indicates that the calcined SiO_2 have more dense Si-O-Si structure and have slow etching kinetics compared to that of the as-synthesized colloidal silica[54]. Since the SiO_2-Au@SiO_2-Cal-NH_3 sample should have PVP-free Au NPs and nanoscale porosity, which can allow molecules to diffuse into the particle, the sample is expected to have higher catalytic activity, stability and excellent recyclability, as discussed next.

The catalytic activity of our SiO_2-Au@SiO_2 samples was evaluated by monitoring the catalytic reduction of 4-NPs with $NaBH_4$ as a reducing agent. The reaction is easy to follow and a good model system to evaluate a metal catalyst because only one main product is generated and the reaction kinetics can be easily determined by measuring the change in the UV-Vis absorbance of the reactant molecule.[22, 44, 59] Figure 4(a) shows the typical absorption spectra for an aqueous 4-NP solution after catalyzing the reduction for various periods using SiO_2-Au@SiO_2-Cal-NH_3 as the catalyst. The strong absorbance peak at 400 nm dramatically decreased and completely disappeared after 300 sec, indicating reduction of 4-NPs. The catalytic performances of the prepared samples are summarized in Figure 4(b). In the blank test (no catalyst), the C/C_0 of 4-NP was reduced by only < 1 % during 300 sec. In addition, we also carried out the 4-NP reduction by using silica sphere (10 mg) to check catalysis of silica. As shown in Figure S3, the typical absorption peak of an aqueous 4-NP solution is continuously maintained during 300 sec and it shows negligible kinetic value in first-order reaction rate plot, indicating that catalysis effect of silica is negligible. However, the 4-NP conversion was significantly enhanced in the presence of the catalysts. The SiO_2-Au catalyst showed the most rapid concentration changes of 4-NPs among the catalysts tested. The extensive exposed Au surface of the SiO_2-Au sample ensured high 4-NP conversion kinetics. However, the SiO_2-Au@SiO_2 catalyst showed the lowest C/C_0 changes with the slowest kinetics during 300 sec because most of the active Au particles were blocked by the outer silica layer additionally deposited. After post-treatments such as calcination and/or etching

with water or diluted ammonia, the catalytic activity of the SiO_2-Au@SiO_2 samples was greatly enhanced. In particular, SiO_2-Au@SiO_2-H_2O and SiO_2-Au@SiO_2-Cal showed ca. 76 and 85 % change in C_t/C_0, respectively, which is much higher than that of as-synthesized SiO_2-Au@SiO_2 (47 %). Among the SiO_2-Au@SiO_2 samples, SiO_2-Au@SiO_2-Cal-NH_3 showed the most enhanced performance, with a C_t/C_0 degradation of > 97% during 300 sec. The relative catalytic activity of the catalysts for 4-NP reduction followed the order: SiO_2-Au> SiO_2-Au@SiO_2-Cal-NH_3> SiO_2-Au@SiO_2-Cal> SiO_2-Au@SiO_2-H_2O> SiO_2-Au@SiO_2.

To compare the reaction kinetics, we re-plotted the previous results to fit the following first-order reaction rate formula: ln (C_t/C_0) = kt. Figure 4c displays the linear relationships of ln (C_t/C_0) versus time (t) in order to facilitate calculation of the reaction kinetic constant. As expected, the blank test showed the smallest rate constant value (0.72×10^{-4} min^{-1}) and the SiO_2-Au catalyst the highest (4.218 min^{-1}) among the tested catalysts. SiO_2-Au@SiO_2 had the lowest kinetic constant among the catalysts but the k values increased through post-treatments such as calcination and/or etching. The rate constant values for 4-NP reduction were 0.24, 0.396, 0.426, and 0.774 min^{-1} for SiO_2-Au@SiO_2, SiO_2-Au@SiO_2-H_2O, SiO_2-Au@SiO_2-Cal and SiO_2-Au@SiO_2-Cal-NH_3, respectively.

As mentioned above, another important issue in heterogeneous metal catalysis is catalytic stability and recyclability. In order to evaluate the catalytic stability and recyclability of the tested catalysts, we carried out multiple runs of catalytic 4-NP reduction. Figure 5 compares the catalytic performances of SiO_2-Au, SiO_2-Au@SiO_2-H_2O, SiO_2-Au@SiO_2-Cal and SiO_2-Au@SiO_2-Cal-NH_3 in five successive cycles of reactions. As expected, the SiO_2-Au catalyst having exposed Au NPs showed high activity in the first cycle. However, the reaction conversion value rapidly dropped in the following cycles of reaction (Figure 5a). Chemical reactions on the Au surface can destabilize the Au-NH_3 interaction so that Au NPs can be gradually detached from the silica surface.[22, 44] As we observed in Figure 1(b), Au NPs are

easily detached and washed out in 4-NP reduction conditions and active sites should be dramatically decreased, resulting in low conversion with repeating reaction cycles. On the other hand, the SiO_2-Au@SiO_2 samples showed well maintained 4-NP conversion values in successive cycles, although the samples showed a small fluctuation within the range of experimental error. Even though the initial 4-NP conversion efficiencies of the SiO_2-Au@SiO_2 catalysts were lower than that of the SiO_2-Au catalyst, they were much more durable over multiple reaction cycles and exhibited a higher conversion ratio in the 5th run. SiO_2-Au@SiO_2-H_2O and SiO_2-Au@SiO_2-Cal showed quite stable conversion values in the range of ca. 74 ~ 79 and 79 ~ 86 %, respectively, during five successive runs, demonstrating the improved recyclability of the Au catalysts attained by depositing a protective silica layer (Figure 5b and c). The SiO_2-Au@SiO_2-Cal-NH_3 sample also showed durable conversion values in the range of 89 - 98 % (Figure 5d). In terms of 4-NP conversion values and stability in the recycling test, the SiO_2-Au@SiO_2-Cal-NH_3 sample showed the highest performance among the tested SiO_2-Au@SiO_2 samples, indicating that it had the most stable recyclability with enhanced activity which was attributed to the post-treatment such as calcination followed by ammonia etching leading to removal of surfactant from the Au surface as well as selective etching of the calcined solid silica to its porous counterpart.

To evaluate the porosity change and surfactant removal, we carried out N_2 adsorption and TGA study. Figure 6 shows the N_2 adsorption-desorption isotherms and corresponding BJH pore size distributions for as-synthesized SiO_2@Au-SiO_2, SiO_2@Au-SiO_2-Cal and SiO_2@Au-SiO_2-Cal-NH_3. SiO_2@Au-SiO_2 and SiO_2@Au-SiO_2-Cal display the main uptake of adsorption at a low relative pressure (0 ~ 0.1 P/P_0) without any obvious adsorption increase in the mesopore range, indicating that they possess highly microporous characteristics,[60] while SiO_2@Au-SiO_2-Cal-NH_3 has a similar uptake at low relative pressure, as well as continuous adsorption uptake in the range of 0.1 ~ 0.7 P/P_0, indicating that it has a

porous structure with both micropores and mesopores[55]. The physical properties of the $SiO_2@Au\text{-}SiO_2$ samples are compared in Table 1. As-synthesized $SiO_2@Au\text{-}SiO_2$ had a micropore surface area and an external surface area of 26 and 20 m^2/g, respectively showing a high micropore ratio (0.57 of S_{micro}/S_{total}). When calcined ($SiO_2@Au\text{-}SiO_2\text{-}Cal$), the micropore surface area was more than doubled and the S_{micro}/S_{total} value increased (0.75), while the external surface area value remained almost constant, indicating that the micropore porosity was dramatically enhanced. After etching with diluted ammonia, $SiO_2@Au\text{-}SiO_2\text{-}Cal\text{-}NH_3$ had a larger external surface area (64.6 m^2/g) and higher ratio of external surface to total surface area (0.6 of $S_{external}/S_{total}$), while the micropore surface area was decreased. This indicates that some of the silica portion was etched out and the micropores were enlarged. It is also confirmed in the pore size distribution results. As shown in Figure 6(b), SiO_2-$Au@SiO_2$ has pores with a size in the range of 10 - 25 Å. SiO_2-$Au@SiO_2$-Cal shows a similar range in pore size distribution, while it has a larger dV/dD value indicating that the microporosity was improved. When the SiO_2-$Au@SiO_2$-Cal sample was etched, the resulted SiO_2-$Au@SiO_2$-Cal-NH_3 showed pores in the range of 10 – 50 Å, indicating that several small micropores were etched out to form bigger mesopores.

Figure 7 show the TGA results for the surfactant (PVP), as-synthesized SiO_2-$Au@SiO_2$, and SiO_2-$Au@SiO_2$-Cal samples. The TGA experiment was conducted using surfactant PVP as a reference run to monitor the decomposition temperature. All TGA runs display weight loss in the range of ambient temperature to ca. 150 ^oC, which is attributed to evaporation of weakly adsorbed H_2O molecules. The TGA curve of PVP shows dramatic weight loss in the range of 300 to 520 ^oC, indicating the thermal oxidation and decomposition of PVP, which is completely burned out after 550 ^oC (Figure 7a). As-synthesized SiO_2-$Au@SiO_2$ displays relatively larger weight loss below 150 ^oC than SiO_2-$Au@SiO_2$-Cal, indicated that the particles have a relative large quantity of water molecules. It shows a steep curve of weight

loss (4 %) in the temperature range of 250 to 500 ^{o}C, indicating that PVP molecules wrapping the surface of embedded Au NPs were burned out and decomposed. However, SiO$_2$-Au@SiO$_2$-Cal shows different thermogravimetric behavior. After a small weight loss in the water desorption region, it doesn't suffer any major weight loss in the range of 250 to 500 ^{o}C, indicating no obvious carbon species in the particle and continuously negligible weight loss (1.1 %) until 700 ^{o}C due to the dehydroxylation process on the silica surface. These results are consistent with the N$_2$ adsorption and reaction results, and support our hypothesis.

4. CONCLUSION

We have demonstrated synthetic methods for preparing SiO$_2$-Au@SiO$_2$ catalysts with embedded Au NPs and a permeable porous silica layer, and investigated their catalytic characteristics. This synthetic method involves Au NP decoration on the surface of silica particles to form Au-SiO$_2$, additional SiO$_2$ coating and finally post-treatments including calcination and/or etching with water or ammonia solution. Even though the SiO$_2$-Au catalyst, with naked Au NPs on the silica surface, displayed high activity in the 1st cycle, other SiO$_2$-Au@SiO$_2$ samples after calcination and/or etching showed better durability with considerably higher and more stable activities. Among the tested catalysts, SiO$_2$-Au@SiO$_2$ prepared by calcination followed by etching with ammonia showed the best performance in terms of activity and recyclability. These results support the conclusion that a key component of achieving high performance and recyclability with excellent stability by using Au NP catalysts is making a clean surface of active Au and a protective porous silica layer that not only allow molecular diffusion but also prevent migration of Au NPs to be sintered. Our synthetic strategy of calcination followed by ammonia etching on SiO$_2$-Au@SiO$_2$ successfully removed surfactant molecules on the Au surface and etched out the dense silica surface in a controllable manner to afford porous structures. We believe that the proposed

strategy is a general and effective method for synthesizing stable noble metal nanocatalysts.

ACKNOWLEDGEMENT

ASSOCIATED CONTENT

Supporting Information. The UV-Vis spectra and digital photo images of various Au NP solutions. Catalysis experimental results in presence of pure silica sphere and derivative weight loss curves for PVP and SiO_2-Au@SiO_2 samples

REFERENCES

1. A. P. Alivisatos, *Science*, 1996, 271, 933-937.
2. M. Bruchez, M. Moronne, P. Gin, S. Weiss and A. P. Alivisatos, *Science*, 1998, 281, 2013-2016.
3. X. Peng, L. Manna, W. Yang, J. Wickham, E. Scher, A. Kadavanich and A. P. Alivisatos, *Nature*, 2000, 404, 59-61.
4. C. B. Murray, D. J. Norris and M. G. Bawendi, *Journal of the American Chemical Society*, 1993, 115, 8706-8715.
5. S. Sun, C. B. Murray, D. Weller, L. Folks and A. Moser, *Science*, 2000, 287, 1989-1992.
6. D. V. Talapin and C. B. Murray, *Science*, 2005, 310, 86-89.
7. H. Lee, S. E. Habas, S. Kweskin, D. Butcher, G. A. Somorjai and P. Yang, *Angewandte Chemie*, 2006, 118, 7988-7992.
8. K. M. Bratlie, H. Lee, K. Komvopoulos, P. Yang and G. A. Somorjai, *Nano Letters*, 2007, 7, 3097-3101.
9. Y. Sun and Y. Xia, *Science*, 2002, 298, 2176-2179.
10. B. Lim, M. Jiang, P. H. C. Camargo, E. C. Cho, J. Tao, X. Lu, Y. Zhu and Y. Xia, *Science*, 2009, 324, 1302-1305.
11. I. E. Maxwell, in *Studies in Surface Science and Catalysis*, eds. W. N. D. E. I. Joe W. Hightower and T. B. Alexis, Elsevier, 1996, vol. Volume 101, pp. 1-9.
12. B. Hammer and J. K. Norskov, *Nature*, 1995, 376, 238-240.
13. B. Hvolbæk, T. V. W. Janssens, B. S. Clausen, H. Falsig, C. H. Christensen and J. K. Nørskov, *Nano Today*, 2007, 2, 14-18.
14. M. Haruta, *Catalysis Surveys from Asia*, 1997, 1, 61-73.
15. M. Haruta, *Catalysis Today*, 1997, 36, 153-166.
16. M. Haruta, N. Yamada, T. Kobayashi and S. Iijima, *Journal of Catalysis*, 1989, 115, 301-309.
17. I. Lee, J. B. Joo, Y. Yin and F. Zaera, *Angewandte Chemie International Edition*, 2011, 50, 10208-10211.
18. R. J. Dillon, J.-B. Joo, F. Zaera, Y. Yin and C. J. Bardeen, *Physical Chemistry Chemical Physics*, 2013, 15, 1488-1496.
19. Z. Ma, S. H. Overbury and S. Dai, *Journal of Molecular Catalysis A: Chemical*, 2007, 273, 186-197.
20. A. Binder, Z.-A. Qiao, G. Veith and S. Dai, *Catalysis Letters*, 2013, 143, 1339-1345.
21. Z. Ma and S. Dai, *ACS Catalysis*, 2011, 1, 805-818.
22. J. Ge, Q. Zhang, T. Zhang and Y. Yin, *Angewandte Chemie International Edition*, 2008, 47, 8924-8928.
23. Y. Liu, J. Goebl and Y. Yin, *Chemical Society Reviews*, 2013, 42, 2610-2653.
24. S. Kim, Y. Yin, A. P. Alivisatos, G. A. Somorjai and J. T. Yates, *Journal of the American Chemical Society*, 2007, 129, 9510-9513.
25. Y. Yin, R. M. Rioux, C. K. Erdonmez, S. Hughes, G. A. Somorjai and A. P. Alivisatos, *Science*, 2004, 304, 711-714.
26. J. B. Joo, Q. Zhang, M. Dahl, F. Zaera and Y. Yin, *Journal of Materials Research*, 2013, 28, 362-368.

27.   J. B. Joo, Q. Zhang, I. Lee, M. Dahl, F. Zaera and Y. Yin, *Advanced Functional Materials*, 2012, 22, 166-174.

28.   J. B. Joo, M. Dahl, N. Li, F. Zaera and Y. Yin, *Energy & Environmental Science*, 2013, 6, 2082-2092.

29.   I. Lee, M. A. Albiter, Q. Zhang, J. Ge, Y. Yin and F. Zaera, *Physical Chemistry Chemical Physics*, 2011, 13, 2449-2456.

30.   C. Gao, Q. Zhang, Z. Lu and Y. Yin, *Journal of the American Chemical Society*, 2011, 133, 19706-19709.

31.   Y. Xu, Y. Zhao, L. Chen, X. Wang, J. Sun, H. Wu, F. Bao, J. Fan and Q. Zhang, *Nanoscale*, 2015.

32.   L. Chen, F. Ji, Y. Xu, L. He, Y. Mi, F. Bao, B. Sun, X. Zhang and Q. Zhang, *Nano Letters*, 2014, 14, 7201-7206.

33.   Q. Zhang, I. Lee, J. Ge, F. Zaera and Y. Yin, *Advanced Functional Materials*, 2010, 20, 2201-2214.

34.   J. B. Joo, R. Dillon, I. Lee, Y. Yin, C. J. Bardeen and F. Zaera, *Proceedings of the National Academy of Sciences*, 2014, 111, 7942-7947.

35.   Q. Zhang, D. Q. Lima, I. Lee, F. Zaera, M. Chi and Y. Yin, *Angewandte Chemie*, 2011, 123, 7226-7230.

36.   J. Joo, Y. Kim, W. Kim, N. Kim, P. Kim, Y. Kim, Y.-W. Lee and J. Yi, *Korean Journal of Chemical Engineering*, 2008, 25, 431-436.

37.   J. B. Joo, Y. J. Kim, W. Kim, P. Kim and J. Yi, *Journal of Nanoscience and Nanotechnology*, 2008, 8, 5130-5134.

38.   H. Yin, H. Tang, D. Wang, Y. Gao and Z. Tang, *ACS Nano*, 2012, 6, 8288-8297.

39.   X.-R. Li, X.-L. Li, M.-C. Xu, J.-J. Xu and H.-Y. Chen, *Journal of Materials Chemistry A*, 2014, 2, 1697-1703.

40.   S.-S. Kim, Y.-R. Kim, T. D. Chung and B.-H. Sohn, *Advanced Functional Materials*, 2014, 24, 2764-2771.

41.   Q. Zhang, I. Lee, J. B. Joo, F. Zaera and Y. Yin, *Accounts of Chemical Research*, 2012.

42.   X. Liang, J. Li, J. B. Joo, A. Gutiérrez, A. Tillekaratne, I. Lee, Y. Yin and F. Zaera, *Angewandte Chemie*, 2012, 124, 8158-8160.

43.   N. Li, Q. Zhang, J. Liu, J. Joo, A. Lee, Y. Gan and Y. Yin, *Chemical Communications*, 2013, 49, 5135-5137.

44.   Y. Hu, Q. Zhang, J. Goebl, T. Zhang and Y. Yin, *Physical Chemistry Chemical Physics*, 2010, 12, 11836-11842.

45.   Q. Zhang, T. Zhang, J. Ge and Y. Yin, *Nano Letters*, 2008, 8, 2867-2871.

46.   P. Angelomé and L. Liz-Marzán, *J Sol-Gel Sci Technol*, 2014, 70, 180-190.

47.   P. C. Angelome, I. Pastoriza-Santos, J. Perez-Juste, B. Rodriguez-Gonzalez, A. Zelcer, G. J. A. A. Soler-Illia and L. M. Liz-Marzan, *Nanoscale*, 2012, 4, 931-939.

48.   P. Botella, A. Corma and M. T. Navarro, *Chemistry of Materials*, 2007, 19, 1979-1983.

49.   P. Botella, A. Corma, M. T. Navarro and M. Quesada, *Journal of Materials Chemistry*, 2009, 19, 3168-3175.

50.   W. Stöber, A. Fink and E. Bohn, *Journal of Colloid and Interface Science*, 1968, 26, 62-69.

51.   X. Han, J. Goebl, Z. Lu and Y. Yin, *Langmuir*, 2011, 27, 5282-5289.

52.   Y. Hu, J. Ge, Y. Sun, T. Zhang and Y. Yin, *Nano Letters*, 2007, 7, 1832-1836.

53.   Q. Zhang, W. Wang, J. Goebl and Y. Yin, *Nano Today*, 2009, 4, 494-507.

54.   J. B. Joo, Q. Zhang, M. Dahl, I. Lee, J. Goebl, F. Zaera and Y. Yin, *Energy & Environmental Science*, 2012, 5, 6321-6327.

55.   J. B. Joo, A. Vu, Q. Zhang, M. Dahl, M. Gu, F. Zaera and Y. Yin, *Chemsuschem*, 2013,

6, 2001-2008.

56. J. B. Joo, I. Lee, M. Dahl, G. D. Moon, F. Zaera and Y. Yin, *Advanced Functional Materials*, 2013, 23, 4246-4254.
57. L. L. Hench and J. K. West, *Chemical Reviews*, 1990, 90, 33-72.
58. G. B. Alexander, W. M. Heston and R. K. Iler, *The Journal of Physical Chemistry*, 1954, 58, 453-455.
59. F.-h. Lin and R.-a. Doong, *The Journal of Physical Chemistry C*, 2011, 115, 6591-6598.
60. J. Joo, P. Kim, W. Kim and J. Yi, *Journal of Electroceramics*, 2006, 17, 713-718.

Table 1. N$_2$ adsorption results indicating total surface area (S$_{total}$), micropore surface area (S$_{micro}$), external surface area (S$_{external}$) and surface area ratios for SiO$_2$@Au-SiO$_2$, SiO$_2$@Au-SiO$_2$-Cal, SiO$_2$@Au-SiO$_2$-Cal-NH$_3$ samples.

Samples	S$_{total}$ (m^2/g)	S$_{micro}$ (m^2/g)	S$_{external}$ (m^2/g)	S$_{micro}$/S$_{total}$	S$_{external}$/S$_{total}$
SiO$_2$@Au-SiO$_2$	46.1	26.2	19.9	0.57	0.43
SiO$_2$@Au-SiO$_2$-Cal	78.6	59.3	19.3	0.75	0.25
SiO$_2$@Au-SiO$_2$-Cal-NH$_3$	108.7	44.1	64.6	0.4	0.6

External surface area (S$_{external}$) means the sum of mesopore surface area, micropore surface area and outer surface area of the particles.
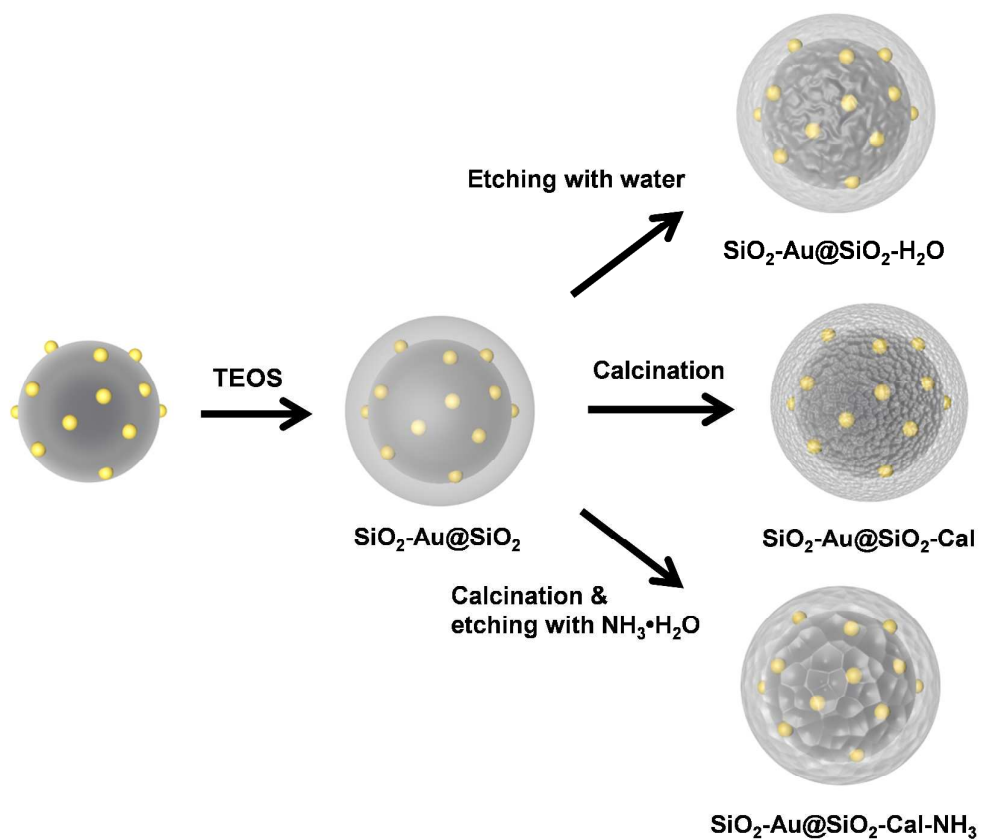
Scheme. 1. Schematic illustration of the fabrication procedure for preparing various SiO_2-Au@SiO_2 catalysts through additional SiO_2 layer coating of SiO_2-Au followed by post-treatments such as calcination and/or etching with water or ammonia

Figures.
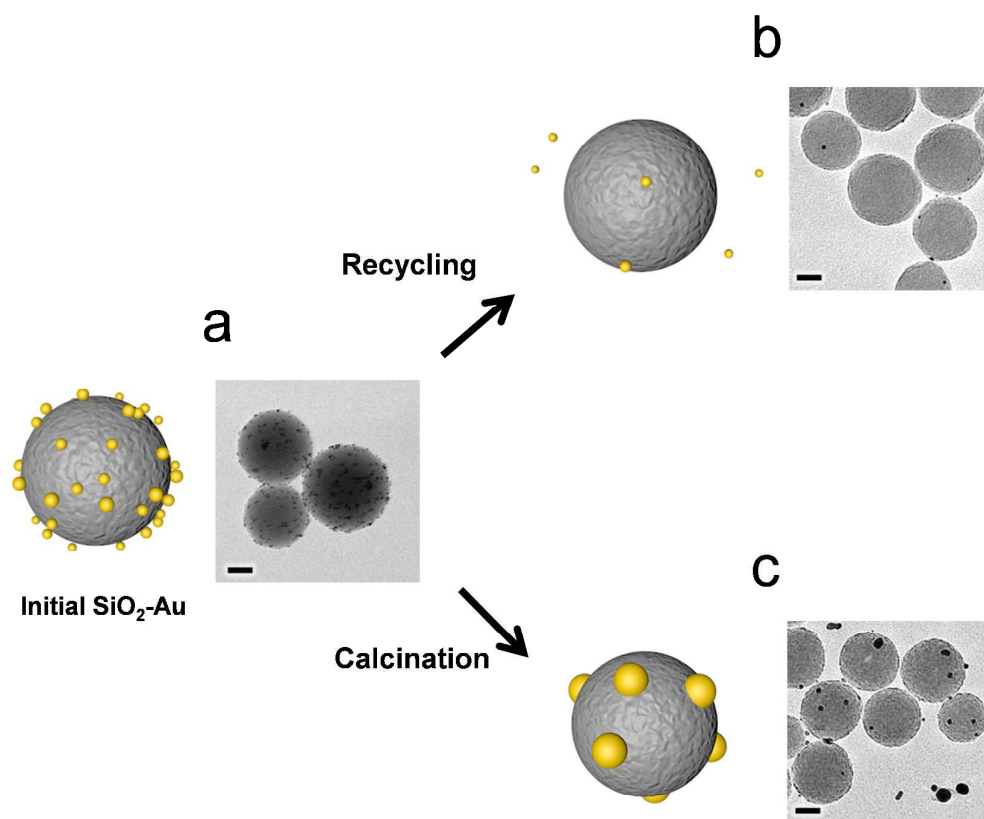
Figure 1. Schematic illustration and corresponding TEM images of (a) initial SiO_2-Au sample, and the samples after (b) catalytic recycling or (c) calcination. All scale bars are 50 nm.
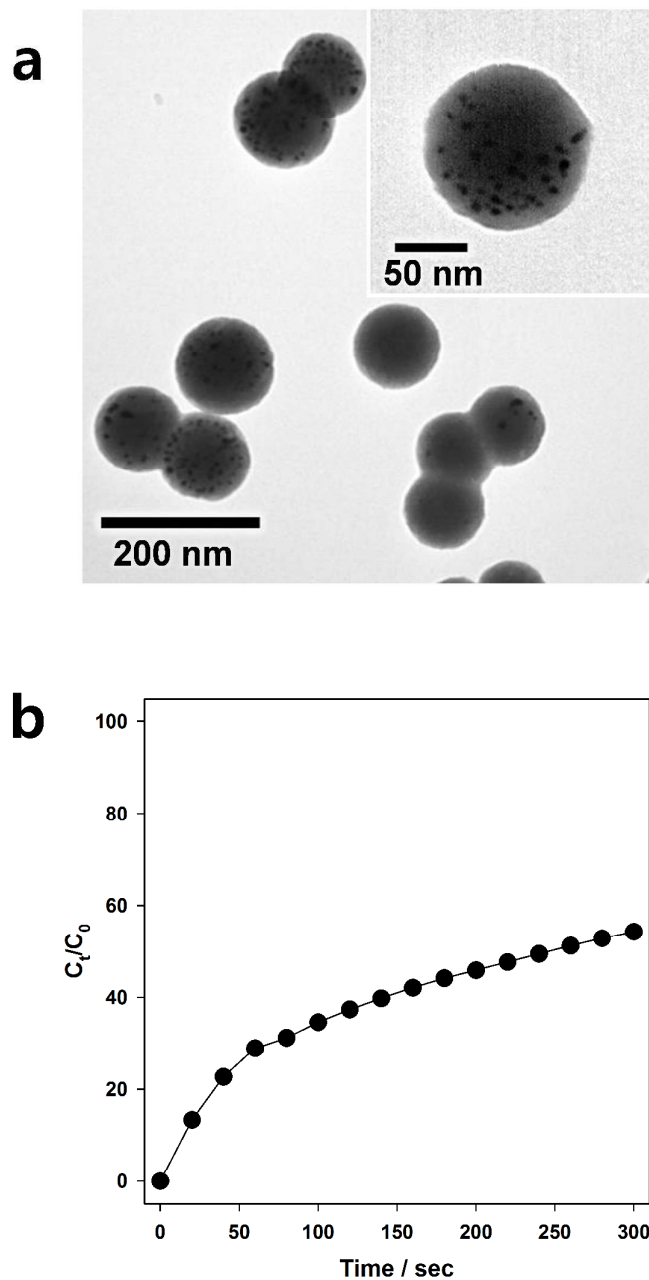
Figure 2.   (a) TEM image and (b) catalytic performance results of as-synthesized SiO_2-Au@SiO_2 samples indicating that most of the Au NPs are covered by an outer silica layer resulting in low 4-NP conversion
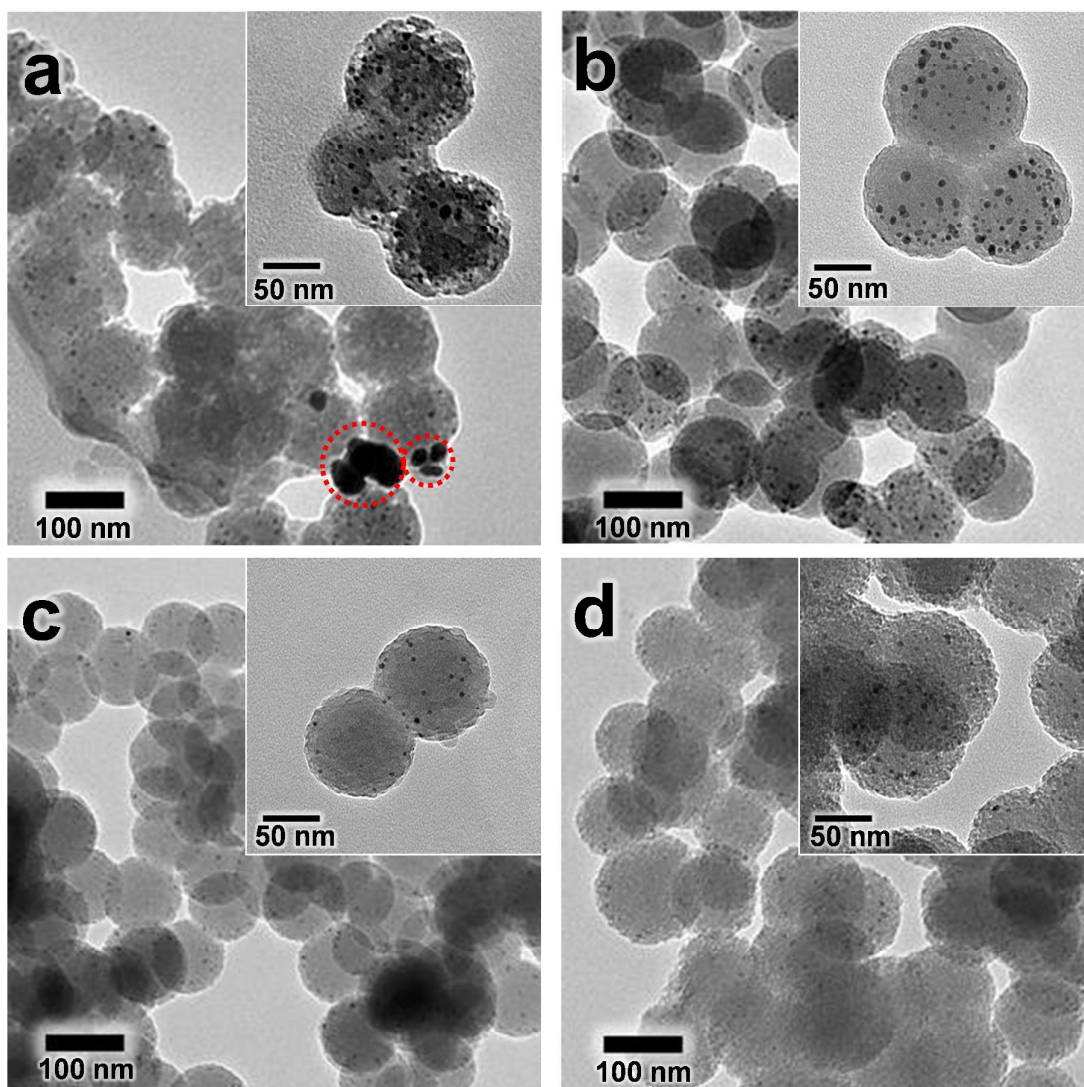
Figure 3. TEM images of SiO_2-Au@SiO_2 samples: (a) SiO_2-Au@SiO_2-NH_3, (b) SiO_2-Au@SiO_2-H_2O, (c) SiO_2-Au@SiO_2-Cal and (d) SiO_2-Au@SiO_2-Cal-NH_3
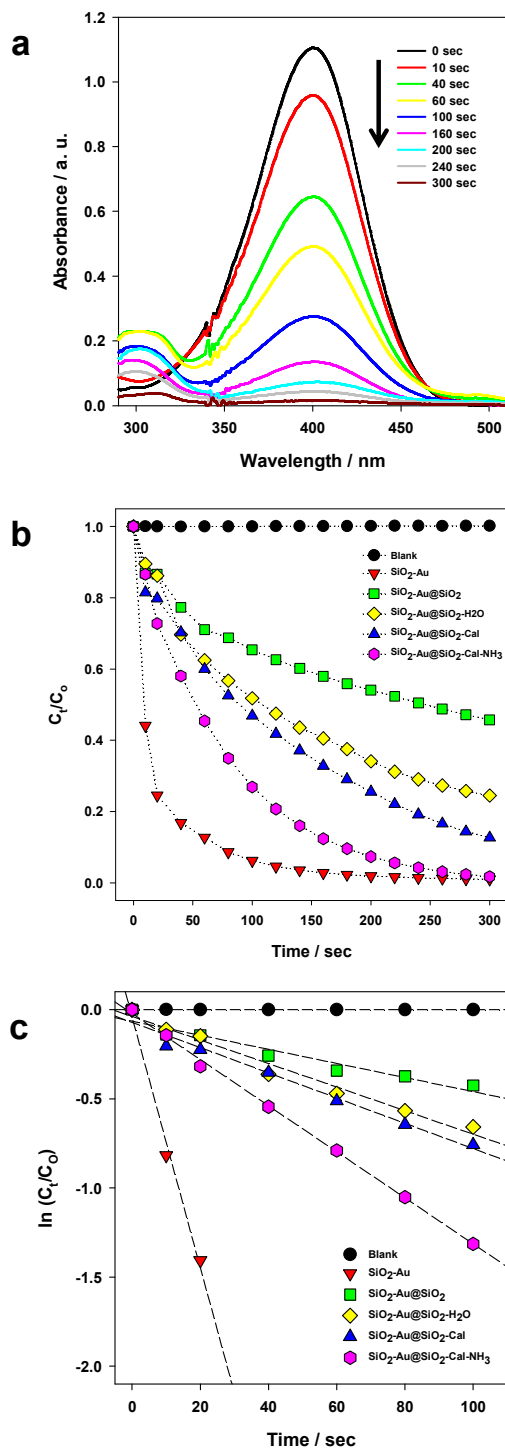
Figure 4. (a) UV-vis absorption spectra changes showing conversion of 4-NP using SiO_2-Au@SiO_2-Cal-NH_3 catalyst, (b) degradation behavior of 4-NP and (c) semi-logarithmic plot versus time in the presence of different catalysts.
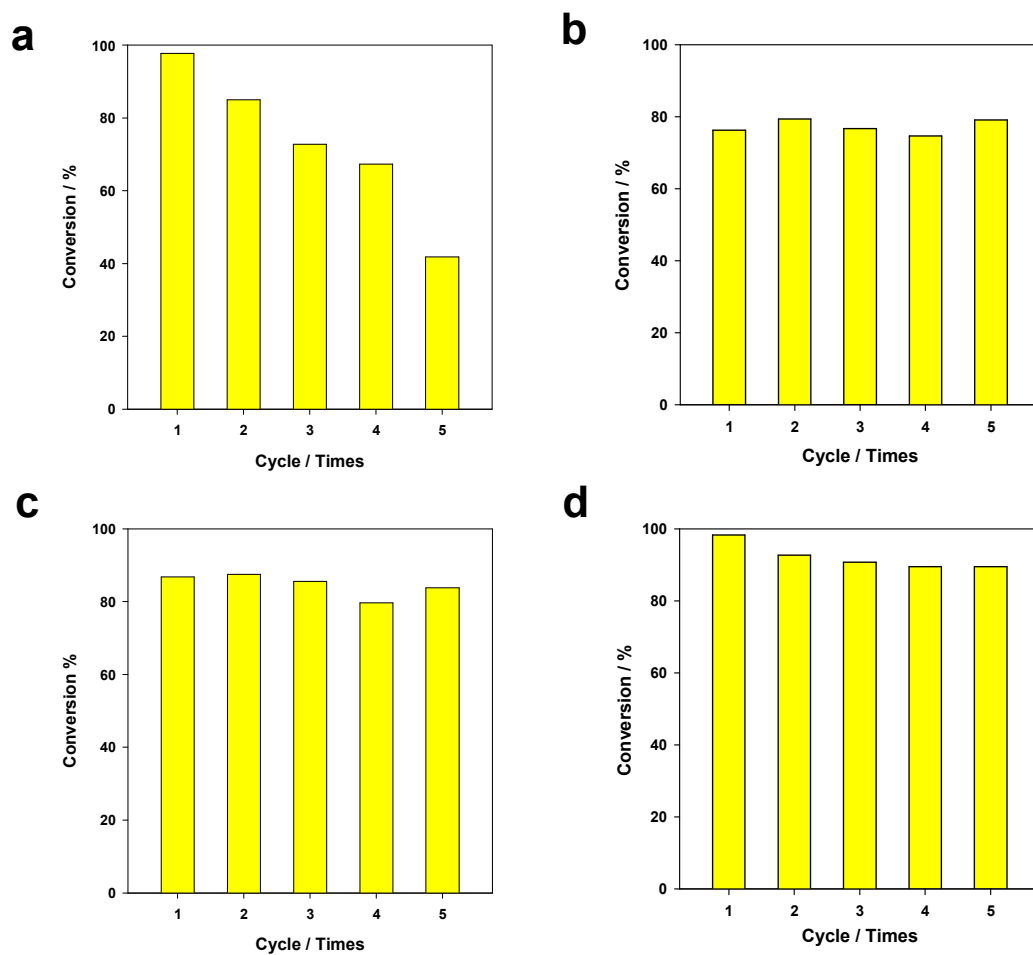
Figure 5. Cycling test results of 4-NP conversion in the presence of different catalysts for 300 sec: (a) SiO$_2$-Au, (b) SiO$_2$-Au@SiO$_2$-H$_2$O, (c) SiO$_2$-Au@SiO$_2$-Cal and (d) SiO$_2$-Au@SiO$_2$-Cal-NH$_3$.
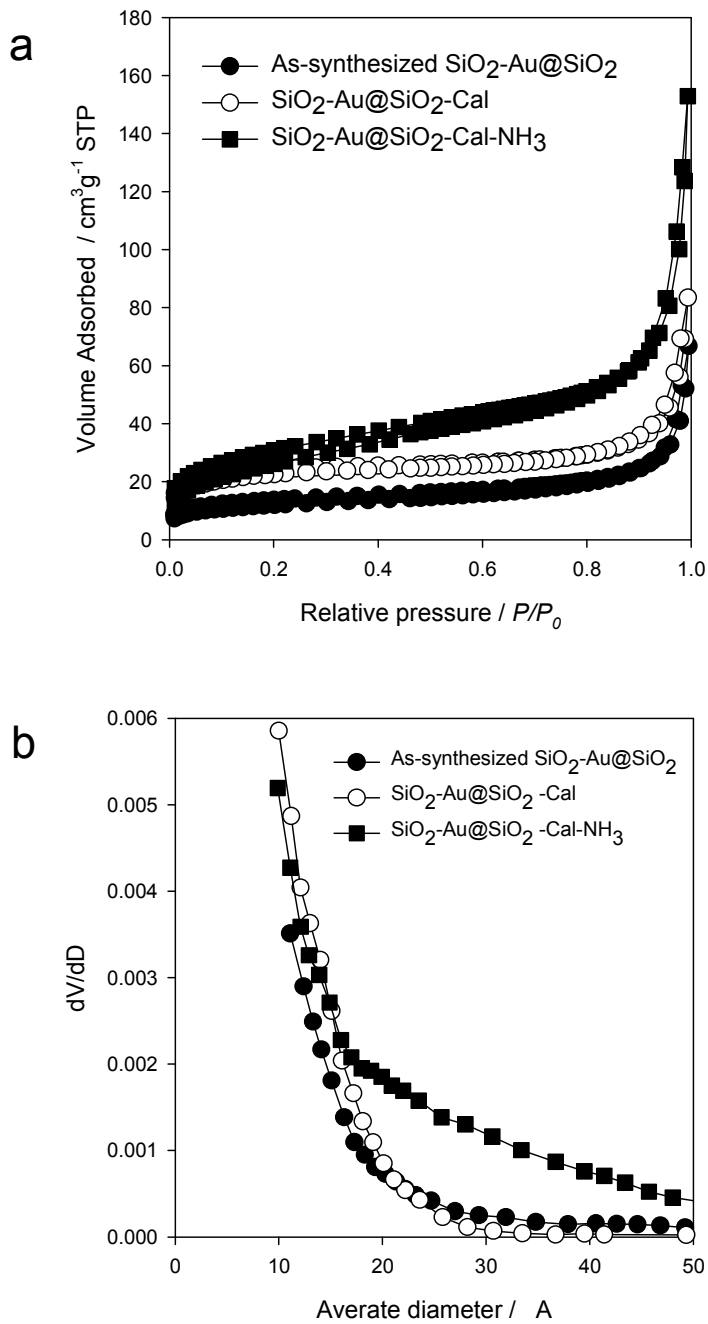
Figure 6. (a) N_2 adsorption-desorption isotherms and (b) corresponding pore size distribution of the SiO_2-Au@SiO_2 catalysts
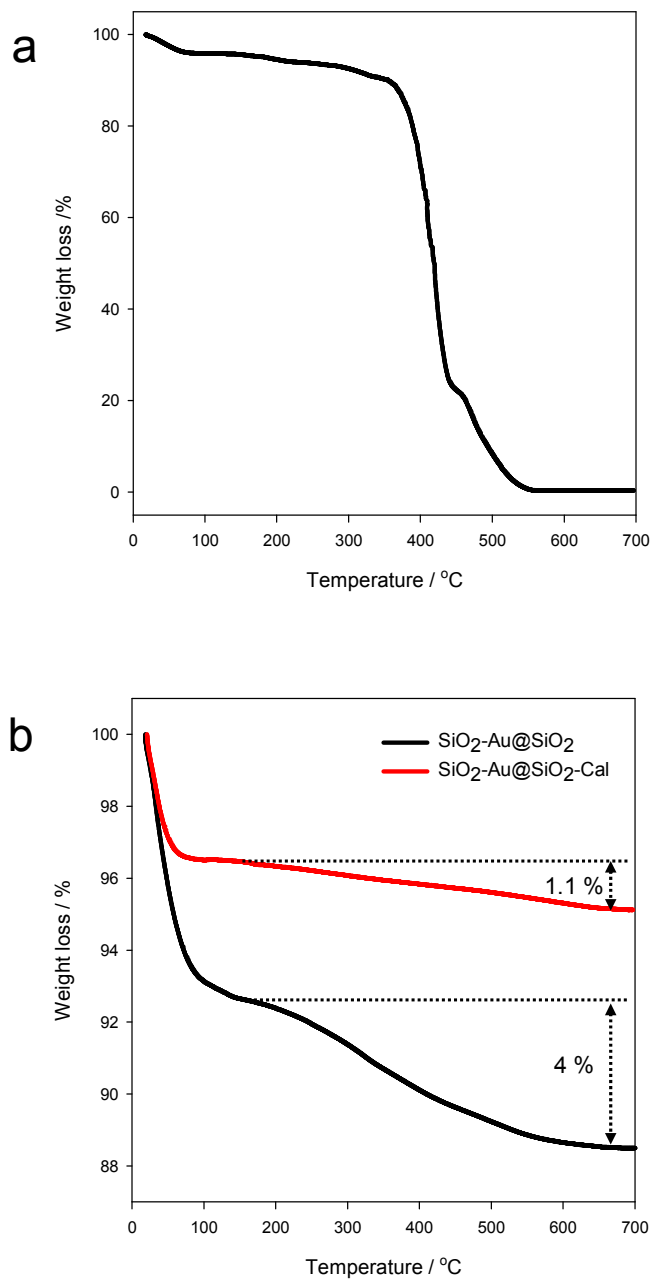
Figure 7. TGA results of (a) PVP decomposition as a reference and (b) SiO_2-Au@SiO_2-Cal and SiO_2-Au@SiO_2 under air conditions.

Graphic Abstract

Au NP-embedded SiO$_2$ (SiO$_2$-Au@SiO$_2$) particles with the improved molecule accessibility, catalyst stability and catalytic performance were successfully synthesized by post-treatments such as calcination and/or etching with water or ammonia.

Post-treatment: calcination and/or etching

**Embedded Au catalyst in
Solid SiO$_2$ shell**

**Embedded Au catalyst in
mesoporous SiO$_2$ shell**